PHOTONIC SENSORS / Vol. 6, No. 3, 2016: 234–242

Optimal Design of 850 nm 2×2 Multimode Interference Polymer Waveguide Coupler by Imprint Technique

Yuchen SHAO[1], Xiuyou HAN[1*], Xiaonan HAN[1], Zhili LU[1], Zhenlin WU[1], Jie TENG[2], Jinyan WANG[3], Geert MORTHIER[4], and Mingshan ZHAO[1]

[1]*School of Physics and Optoelectronic Engineering, Dalian University of Technology, Dalian, 116024, China*

[2] *No. 38 Research Institute, China Electronics Technology Group Corporation, Hefei, 230088, China*

[3] *School of Chemical Engineering, Dalian University of Technology, Dalian, 116024, China*

[4]*Photonics Research Group, Department of Information Technology, Ghent University-IMEC, 9000 Ghent, Belgium*

[*]Corresponding author: Xiuyou HAN E-mail: xyhan@dlut.edu.cn

Abstract: A 2×2 optical waveguide coupler at 850 nm based on the multimode interference (MMI) structure with the polysilsesquioxanes liquid series (PSQ-Ls) polymer material and the imprint technique is presented. The influence of the structural parameters, such as the single mode condition, the waveguide spacing of input/output ports, and the width and length of the multimode waveguide, on the optical splitting performance including the excess loss and the uniformity is simulated by the beam propagation method. By inserting a taper section of isosceles trapezoid between the single mode and multimode waveguides, the optimized structural parameters for low excess loss and high uniformity are obtained with the excess loss of –0.040 dB and the uniformity of –0.007 dB. The effect of the structure deviations induced during the imprint process on the optical splitting performance at different residual layer thicknesses is also investigated. The analysis results provide useful instructions for the waveguide device fabrication.

Keywords: Polymer waveguide; coupler; multimode interference

Citation: Yuchen SHAO, Xiuyou HAN, Xiaonan HAN, Zhili LU, Zhenlin WU, Jie TENG, *et al*., "Optimal Design of 850 nm 2×2 Multimode Interference Polymer Waveguide Coupler by Imprint Technique," *Photonic Sensors*, 2016, 6(3): 234–242.

1. Introduction

The optical waveguide coupler, as a basic unit, implements the function of splitting or combining lightwave in photonic integrated circuits. Compared with the conventional directional coupler, the coupler based on the multimode interference (MMI) structure has many advantages including compact structure, good fabrication tolerance, low optical loss, and polarization insensitivity [1–3]. The MMI based coupler can constitute the high speed optical switch [4, 5], large extinct ratio modulator [6], high Q waveguide microring filter [7], multi-wavelength laser array [8], and compact optical 90° hybrid for a balanced detection receiver [9].

Among the optical materials for integrated waveguide devices, the polymer has the features of low cost, flexible tuning of refractive index, and easy forming of film by spin-coating [10]. The polymer based integrated waveguide devices can be fabricated by the simple imprint technique [11], which avoids the complicated processes of growth and etching for fabrication of inorganic optical

Received: 6 May 2016 / Revised: 25 May 2016

DOI: 10.1007/s13320-016-0341-9
Article type: Regular

waveguide devices with silicon, silica or semiconductor materials. Also, polymer waveguide devices can be integrated with a light source and a photo detector on a common board, which promote the reduction in cost and minimization of the optical module and subsystem [12, 13]. The research on polymer based optical waveguide devices has been attracting more and more attention in the field of optical interconnection on board [14], high speed coherent receiver [15], and optical biosensor [16, 17]. Especially for the optical biosensor, the polymer materials have several unique advantages. Among these, polymer surfaces have good biocompatibility and can be easily modified to immobilize a wide range of biomolecules, which is beneficial to achieve the label-free detection [18]. Additionally, most analytes are aqueous with a large optical absorption loss at the lightwave band of 1550 nm, which greatly deteriorates the performance of silicon on insulator based biosensors [19]. The polymer waveguides can work at the lightwave bands of 650 nm or 850 nm [20–22] where the aqueous analytes have a very low optical absorption loss [23].

Many researches on the polymer waveguide MMI coupler have been carried out [23–28], which are generally around 1550 nm. In this paper, the MMI based 2×2 optical waveguide coupler at 850 nm with the polysilsesquioxanes liquid series (PSQ-Ls) polymer material [29] and the imprint technique [30] is optimally designed. The influence of the structural parameters such as the single mode conditions, the waveguide spacing of input/output waveguides, and the width and length of the multimode waveguide, on the device performance including the excess loss and the uniformity, is simulated and analyzed. The optimized structural parameters for low excess loss and high uniformity are obtained. The influence of the structural parameter deviations induced during the imprint process on the device performance under different residual layer thicknesses is also studied. The analysis results provide useful instructions for the following waveguide device fabrication.

2. Structure design

Figure 1 shows the 2×2 optical waveguide coupler based on the MMI structure, which has two input single mode waveguides: (1) the multimode waveguide and (2) output single mode waveguides. The single mode conditions of input/output waveguides, the waveguide spacing D, and the width W_{MMI} and length L_{MMI} of the multimode waveguide are the main structural parameters to be designed.

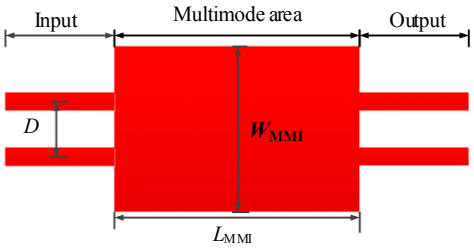

Fig. 1 2×2 optical waveguide coupler based on the MMI structure.

The excess loss and the uniformity are the two important performance indices of the coupler, with the unit of dB. The excess loss is defined as [31]

$$EL = 10\lg\left(\frac{\sum P_{\mathrm{out}}}{\sum P_{\mathrm{in}}}\right) \tag{1}$$

where $\sum P_{\mathrm{out}}$ is the sum of output optical power, and $\sum P_{\mathrm{in}}$ is the sum of input optical power.

The uniformity is defined as [31]

$$UF = 10\lg\left(\frac{P_{\min}}{P_{\max}}\right) \tag{2}$$

where $P_{\min}$ and $P_{\max}$ are the minimum and maximum optical powers of the two output ports, respectively.

The structure model of the 2×2 coupler based on MMI is built and simulated by the beam propagation method (BPM). The wavelength of the input optical field is set as 850 nm, and the input power is normalized as 1. The power of two output ports is monitored when the waveguide structural parameters, such as the waveguide spacing D, the

width W_{MMI}, and length L_{MMI} of the multimode waveguide, are adjusted. Then the excess loss and uniformity are calculated with (1) and (2). The structural parameters are optimized by simulating the influence of the different structural parameters on the excess loss and the uniformity.

2.1 Waveguide cross section

Figure 2 shows the cross section of the input/output waveguide of the MMI based coupler. The material of the lower cladding is the PSQ-Ls with the low index of 1.458 named as PSQ-LL, and the core is the PSQ-Ls with the high index of 1.529 named as PSQ-LH [29]. The upper cladding is set as air with the index of 1. As well known, the height H and width W of the core should fulfill the single mode condition. In addition, the residual layer with the thickness of Δh will be generated when the core is fabricated by the imprint technique [30], and the influence of the residual layer on the performance of the coupler could not be ignored.

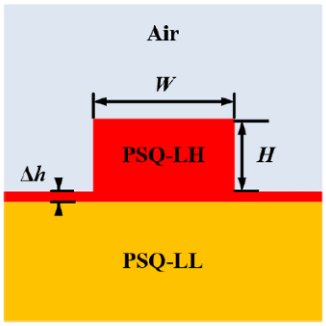

Fig. 2 Schematic of the input/output waveguide cross section.

Figure 3 shows the effective refractive index versus different widths W of the core with the height of the core H=1 μm and he thickness of the residual layer Δh=0.2 μm, respectively. It can be seen from Fig. 3 that the higher-order mode will appear when the width is equal to or larger than 2 μm. Therefore, the width of the core is chosen as 1.8 μm. The inset of Fig. 3 shows the calculated mode field with the core width of 1.8 μm. It can be seen clearly that only the fundamental mode transmits in the waveguide.

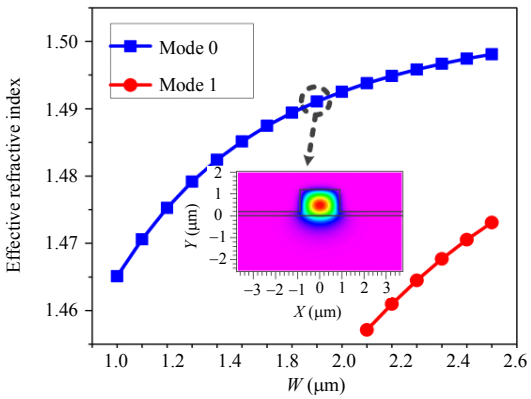

Fig. 3 Effective refractive index versus different waveguide core widths.

2.2 Waveguide spacing

The mode coupling occurs when the two waveguides are close to each other, which impacts the optical splitting property of the MMI based coupler. The model of two parallel straight waveguides with the length of 500 μm is set up as the inset in Fig. 4. The lightwave field with the normalized power of 1 is input to Waveguide 1, and the output power from Waveguide 2 is monitored when the waveguide spacing D changes.

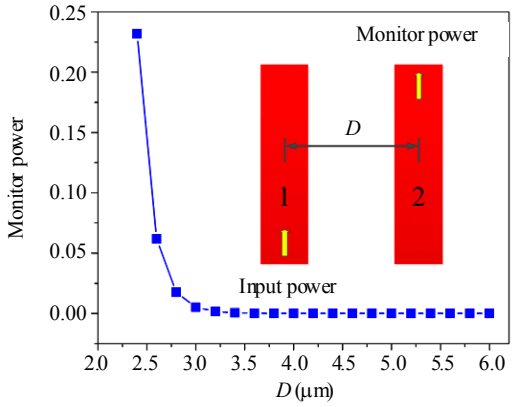

Fig. 4 Power output from Waveguide 2 versus different waveguide spacings D.

Figure 4 shows the output power from Waveguide 2 versus different waveguide spacings D. The lightwave power coupled from Waveguide 1 into Waveguide 2 gradually decreases with an increase in the waveguide spacing D, and the power approaches zero when the waveguide spacing increases to 3.4 μm. The power does not change as the waveguide spacing further increases. The waveguide

spacing D of the input/output waveguides is chosen as 5 μm in consideration of no coupling between the two parallel waveguides and the feasibility of the waveguide fabrication with the imprint technique.

2.3 Multimode waveguide

For the multimode waveguide design, the width W_{MMI} and length L_{MMI} of the waveguide are the main structural parameters. The two input/output waveguides of the 2×2 MMI based coupler with 3-dB splitting ratio are located at $W_e/3$ and $2W_e/3$ of the multimode waveguide, respectively, according to the self-image principle [31]. The effective width of the waveguide is defined as W_e and is approximately equal to the practical width of the waveguide:

$$W_{\mathrm{MMI}} \approx W_e = 3D. \tag{3}$$

The length of the multimode waveguide meets the following relationship:

$$L_{\mathrm{MMI}} = \frac{1}{2}L_\pi = \frac{1}{2}\frac{4n_{\mathrm{core}}W_e^2}{3\lambda_0} \approx \frac{2n_{\mathrm{core}}W_{\mathrm{MMI}}^2}{3\lambda_0} \tag{4}$$

where L_π is the beat length of the two lowest-order modes, n_{core} is the index of the waveguide core, λ_0 is the wavelength of the input lightwave. With the above chosen waveguide spacing D of 5 μm, the width of the multimode waveguide is about 15 μm, and the length of the multimode waveguide is about 270 μm according to (3) and (4), respectively.

Then the model of the 2×2 MMI based coupler is established according to above parameters. The excess loss and uniformity are simulated and calculated when the input/out waveguide spacing D is tuned with a step of 0.1 μm. Figure 5(a) shows the excess loss and uniformity with different spacings D. Obviously, the change in the waveguide spacing has the primary influence on the excess loss which approaches the minimum as D is 5.1 μm. Figure 5(b) shows the excess loss and uniformity with different the multimode waveguide lengths L_{MMI}. It can be seen that the excess loss approaches the minimum as L_{MMI} is 273 μm. Therefore, the width W_{MMI} and length L_{MMI} of the multimode waveguide are chosen as 5.1 μm and 273 μm, respectively.

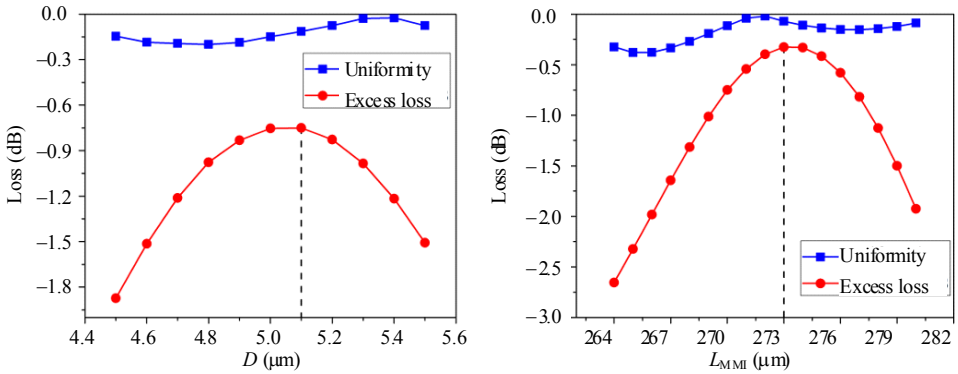

Fig. 5 Excess loss and uniformity: (a) different input/output waveguide spacings D and (b) different lengths of the multimode waveguide L_{MMI}.

The optical splitting property of the 2×2 MMI based coupler is simulated with above structural parameters, and the result is shown in Fig. 6. From Fig. 6, it can be observed that the normalized power of two output ports is 0.4712 and 0.4647, respectively. Then the excess loss is –0.325 dB, and the uniformity is –0.071 dB calculated by (1) and (2). The structural parameters and performance indices of the 2×2 MMI based coupler are listed in Table 1.

Table 1 Structural parameters and performance indices of the 2×2 MMI optical waveguide coupler.

W	H	D	W_{MMI}	L_{MMI}	EL	UF
1.8μm	1μm	5.1μm	15μm	273μm	–0.325dB	–0.071dB

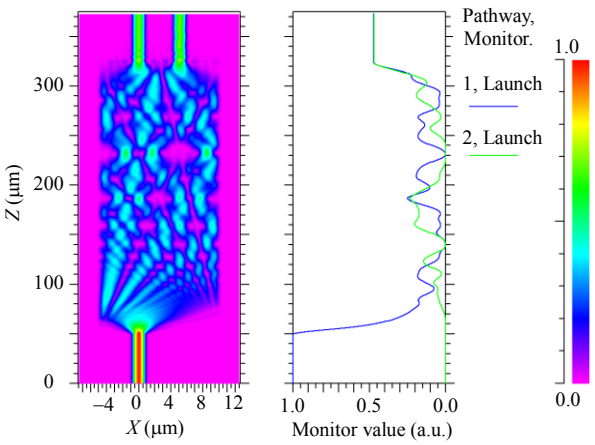

Fig. 6 BPM simulation result of the 2×2 MMI based coupler.

3. Structure optimization

From Table 1, it can be seen that the excess loss of the 2×2 MMI based coupler is relatively high. It is due to the mismatch loss between the single mode and multimode waveguides. A taper section of isosceles trapezoid with the length L_{taper} and the width W_{taper}, as shown in Fig. 7, is inserted between the single mode and multimode waveguides to suppress the mismatch loss [32, 33].

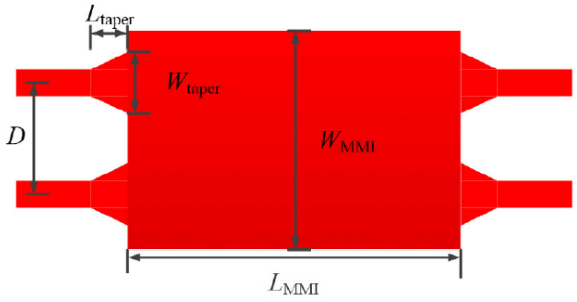

Fig. 7 2×2 MMI based coupler with the taper section.

The structural parameters of the taper section are optimized. At first, the excess loss with different widths W_{taper} of the taper section is simulated with the length L_{taper} of 100 μm, and the result is shown in Fig. 8(a). The excess loss decreases gradually with an increase in the width W_{taper}. It tends to be the minimum when W_{taper} is 3.1 μm, and it doesn't change basically when W_{taper} increases further. Then the width W_{taper} of the taper section is selected as 3.1 μm to analyze the excess loss with different lengths L_{taper} of the taper section, and the result is shown in Fig. 8(b). L_{taper} is selected as 100 μm to ensure the minimum excess loss with the possible short length of the taper section.

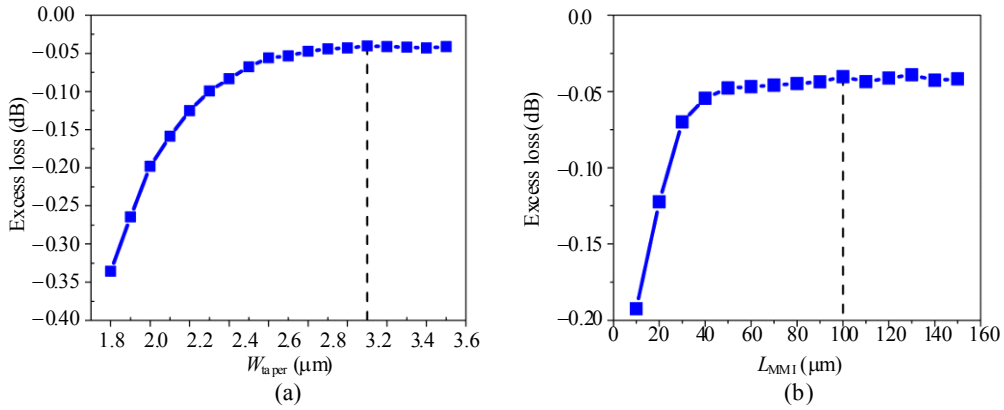

Fig. 8 Excess loss with different widths W_{taper} (a) and lengths L_{taper} (b) of the taper section.

The optical splitting performance of the 2×2 MMI based coupler is simulated with the optimized structural parameters, and the result is shown in Fig. 9. The normalized powers of two output ports are 0.4949 and 0.4958, respectively. Then the excess loss is –0.040 dB, and the uniformity is –0.007 dB calculated by (1) and (2). The structure and property parameters of the optimized coupler are listed in Table 2. Comparing the parameters between Tables 1 and 2, the excess loss is reduced obviously after introducing the taper section between single mode and multimode waveguides. At the same time, the uniformity is also improved significantly.

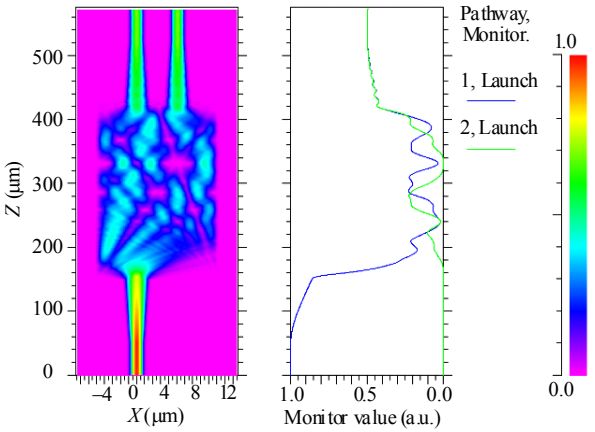

Fig. 9 Simulated result of the 2×2 MMI based coupler with the taper section.

Table 2 Structural parameters and performance indices of the 2×2 MMI based coupler with the taper section.

W	H	D	W_{MMI}	L_{MMI}	W_{taper}	L_{taper}	EL	UF
1.8μm	1μm	5.1μm	15μm	273μm	3.1μm	100μm	–0.040dB	–0.007dB

4. Discussion of fabrication tolerance

The optimized 2×2 MMI based coupler has the good characteristics of optical splitting, but the structural parameters such as the waveguide spacing D, length L_{MMI}, and width W_{MMI} of the multimode waveguide may deviate from the optimal values due to the horizontal offset of the mold during the fabrication process by the imprint technique. At the same time, the thickness of the residual layer may vary in a small range due to the tiny change in pressure, which also exerts negative effect on the optical splitting performance of the coupler. Therefore, it is necessary to analyze the structural parameter tolerance of the coupler to give instructions for the device fabrication and performance improvement.

At first, the influence of deviation of the multimode waveguide width W_{MMI} from the optimized value on the excess loss and the uniformity is analyzed. The input/output waveguide spacing D and the length L_{MMI} of the multimode waveguide are set as the optimized values of D = 5.1 μm and L_{MMI} = 237 μm. The thickness of the residual layer is set as 0.1 μm, 0.2 μm, and 0.3 μm, respectively. The power from the two output ports of the coupler are obtained by simulation with the BPM, with which the excess loss and uniformity are calculated by (1) and (2). The analysis results are shown in Fig. 10. It can be seen that the deviations of the multimode waveguide width W_{MMI} have a larger influence on the excess loss than on the uniformity. For the excess loss, as shown in Fig. 10(a), it increases gradually as W_{MMI} deviates from the optimized value. The changes in the residual layer thickness Δh also affect the excess loss a bit. However, it would be acceptable if the deviation of W_{MMI} is in a certain range. The maximum values of the excess loss and uniformity are set as –0.3 dB and –0.1 dB, respectively. The tolerable deviation of W_{MMI} is between –0.1 μm and 0.12 μm (0.67%) from the optimized value of 15 μm.

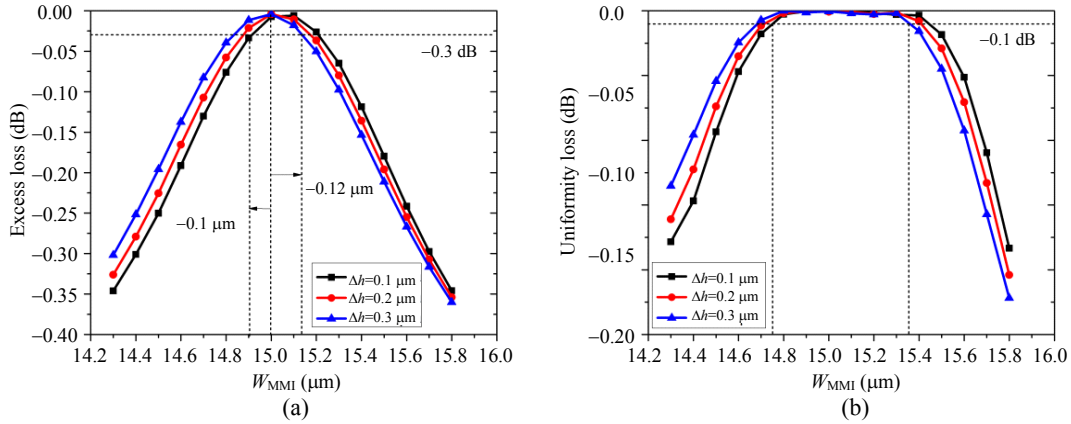

Fig. 10 Splitting performance: (a) excess loss and (b) uniformity with different W_{MMI} at different thicknesses of the residual layer.

Then the influence of deviations of the multimode waveguide length L_{MMI} and the waveguide spacing D of the input/output port from the optimized values on the excess loss and uniformity is analyzed by the similar process. The analysis results are shown in Figs. 11 and 12, respectively. For the maximum values of excess loss and uniformity of –0.3 dB and –0.1 dB, the tolerable deviation of L_{MMI} is between –5 μm and 3 μm (1.10%) from the optimized value of 273 μm, and the tolerable deviation of D is between –0.44 μm and 0.35 μm (6.86%) from the optimized value of 5.1 μm.

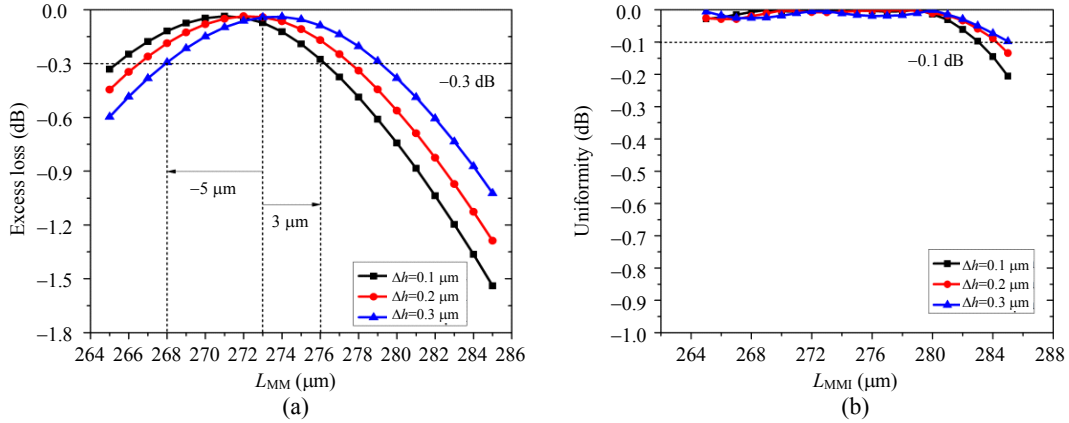

Fig. 11 Splitting performance: (a) excess loss and (b) uniformity with different L_{MMI} at different thicknesses of the residual layer.

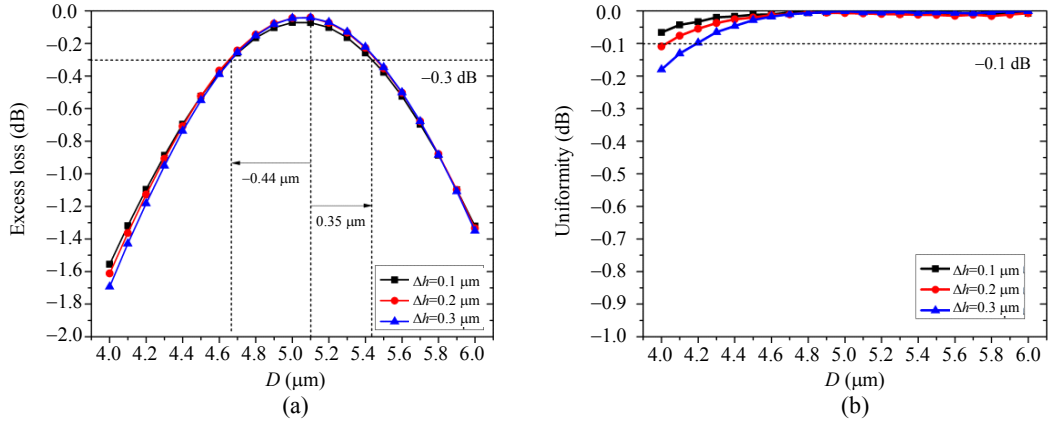

Fig. 12 Splitting performance: (a) excess loss and (b) uniformity with different D at different thicknesses of the residual layer.

According to the above analysis, the length L_{MMI} and the width W_{MMI} of the multimode waveguide have less tolerance than the waveguide spacing D of the input/output port. Therefore, they should be controlled precisely during the waveguide fabrication process. On the other hand, the thickness of the residual layer Δh could be a favorable measure to improve the performance of the coupler. For example, Δh could increase properly in the fabrication process if the practical L_{MMI} is larger than the designed value. Overall, the structural parameters of the 2×2 MMI based coupler, such as the waveguide spacing D, the length L_{MMI}, the width W_{MMI} of the multimode waveguide, and the residual layer thickness Δh should be considered comprehensively in order to improve the performance of the coupler.

5. Conclusions

A 2×2 MMI based optical waveguide coupler at 850 nm with the polymer of PSQ-Ls and imprint technique has been optimally designed by the BPM. The height and width of the waveguide core for single mode transmission is designed as 1 μm and

1.8 μm, respectively. The optimized structural parameters including the waveguide spacing D of the input/output port, the length L_{MMI}, and the width W_{MMI} of the multimode waveguide are obtained by minimizing the excess loss and uniformity and inserting the taper section of isosceles trapezoid between the single mode and multimode waveguides. The excess loss and the uniformity of the MMI based coupler are –0.040 dB and –0.007 dB, respectively, with the optimized structural parameters. The fabrication tolerance of structural parameters has also been investigated in order to achieve an MMI based coupler with good performance by the imprint technique. The analysis results provide useful instructions for the further waveguide device fabrication.

Acknowledgment

This work was supported in part by the International Science & Technology Cooperation Program of China (No. 2014DFG32590), National Natural Science Foundation of China (No.61077015, 61307040), National R&D Program (No.2012AA040406), Natural Science Foundation of Liaoning Province (No. 2014020002), Opening Project of Shanghai Key Laboratory of All Solid-state Laser and Applied Techniques (No. 2013ADL04), and Fundamental Research Funds for the Central Universities (DUT13JB01, DUT15ZD231, and DUT2015TD47).

Reference

[1] L. W. Cahill and T. T. Le, "Optical signal processing using MMI elements," in *10th Anniversary International Conference on Transparent Optical Networks*, Greece, vol. 4, pp. 114–117, 2008.

[2] H. F. Zhou, J. F. Song, C. Li, H. J. Zhang, and P. G. Lo, "A library of ultra-compact multimode interference optical couplers on SOI," *IEEE Photonics Technology Letter*, 2013, 25(12): 1149–1152.

[3] L. Lu, L. Zhou, S. Li, Z. Li, X. Li, and J. Chen, "4 × 4 nonblocking silicon thermo-optic switches based on multimode interferometers," *Journal of Lightwave Technology*, 2015, 33(4): 857–864.

[4] N. Xie, T. Hashimoto, and K. Utaka, "Very low-power, polarization-independent, and high-speed polymer thermooptic switch," *IEEE Photonics Technology Letters*, 2009, 21(24): 1861–1863.

[5] A. M. Al-Hetar, A. B. Mohammad, A. S. M. Supa'at, and Z. A. Shamsan, "MMI-MZI polymer thermo-optic switch with a high refractive index contrast," *Journal of Lightwave Technology*, 2011, 29(2): 171–178.

[6] R. W. Chuang, M. T. Hsu, Y. C. Chang, Y. J. Lee, and S. H. Chou, "Integrated multimode interference coupler-based Mach-Zehnder interferometric modulator fabrication a silicon-on-insulator substrate," *IET Optoelectronics*, 2012, 6(3): 147–152.

[7] L. Jin, J. W. Wang, X. Fu, B. Yang, Y. C. Shi, and D. X. Dai, "High-Q microring resonators with 2 × 2 angled multimode interference couplers," *IEEE Photonics Technology Letters*, 2013, 25(6): 612–614.

[8] J. P. Leidner and J. R. Marciante, "Tapered multi-mode interference waveguide for high-power self-organizing single-mode semiconductor laser arrays," *IEEE Journal Quantum Electronics*, 2011, 47(7): 965–971.

[9] S. H. Jeong and K. Morito, "Compact optical 90° hybrid employing a tapered 2×4 MMI coupler serially connected by a 2×2 MMI coupler," *Optics Express*, 2010, 18(5): 4275–4288.

[10] H. Ma, A. K. Y. Jen, and L. R. Dalton, "Polymer-based optical waveguides: materials, processing, and devices," *Advanced Materials*, 2002, 14(19): 1339–1365.

[11] L. J. Guo, "Recent progress in nanoimprint technology and its applications," *Journal of Physics D: Applied Physics*, 2004, 37(11): R123–R141.

[12] J. Wang, C. Zawadzki, N. Mettbach, W. Brinker, Z. Y. Zhang, D. Schmidt, *et al.*, "Polarization insensitive 25-Gbaud direct D(Q)PSK receiver based on polymer planar lightwave hybrid integration platform," *Optics Express*, 2011, 19(13): 12197–12207.

[13] Z. Zhang, A. Maese-Nove, A. Polatynski, T. Mueller, G. Irmscher, D. Felipe, *et al.*, "Colorless, dual-polarization 90° hybrid with integrated VOAs and local oscillator on polymer platform," in *Optical*

Fiber Communications Conference and Exhibition, California, vol. TH1F3, pp.1–3, 2015.

[14] N. Bamiedakis, A. Hashim, R. V. Penty, and I. H. White, "A 40 Gb/s optical bus for optical backplane interconnections," *Journal of Lightwave Technology*, 2014, 32(8): 1526–1537.

[15] J. Wang, M. Kroh, A. Theurer, C. Zawadzki, D. Schmidt, R. Ludwig, *et al*., "Dual-quadrature coherent receiver for 100G Ethernet applications based on polymer planar lightwave circuit," *Optics Express*, 2011, 19(26): B166–B172.

[16] L. Wang, J. Ren, X. Han, T. Class, X. Jian, P. Bienstman, *et al*., "A label-free optical biosensor built on a low cost polymer platform," *IEEE Photonics Journal*, 2012, 4(3): 920–930.

[17] C. Delezoide, M. Salsac, J. Lautru, H. Leh, C. Nogues, J. Zyss, *et al*., "Vertically coupled polymer micro-racetrack resonators for label-free biochemical sensors," *IEEE Photonics Technology Letters*, 2012, 24(4): 270–272.

[18] J. Ren, L. Wang, X. Han, J. F. Cheng, H. L. Lv, J. Y. Wang, *et al*., "Organic silicone sol-gel polymer as non-covalent carrier of receptor proteins for label-free optical biosensor application," *ACS Applied Materials & Interfaces*, 2013, 5(2): 386–894.

[19] S. Schmidt, J. Flueckiger, W. X. Wu, S. M. Grist, S. T. Fard, V. Donzella, *et al*., "Improving the performance of silicon photonic rings, disks, and Bragg gratings for use in label-free biosensing," *SPIE*, 2014, 9166(91660M): 1–38.

[20] M. H. Salleh, A. Glidle, M. Sorel, J. Reboud, and J. M. Cooper, "Polymer dual ring resonators for label-free optical biosensing using microfluidics," *Chemical Communications*, 2013, 49(30): 3095–3097.

[21] J. Halldorsson, N. B. Arnfinnsdottir, A. B. Arnfinnsdottir, B. Agnarsson, and K. Leosson, "High index contrast polymer waveguide platform for integrated biophotonics," *Optics Express*, 2010, 18(15): 16217–16226.

[22] X. B. Wang, J. Sun, Y. F. Liu, J. W. Sun, C. M. Chen, X. Q. Sun, *et al*., "650-nm 1×2 polymeric thermo-optic switch with low power consumption," *Optics Express*, 2014, 22(9): 11119–11128.

[23] L. Kou, D. Labrie, and P. Chylek, "Refractive indices of water and ice in the 0.65- to 2.5-μm spectral range," *Applied Optics*, 1993, 32(19): 3531–3540.

[24] F. Wang, J. Y. Yang, L. M. Chen, X. Q. Jiang, and M. H. Wang, "Optical switch based on multimode interference coupler," *IEEE Photonics Technology Letters*, 2006, 18(2):421–423.

[25] L. Yang, B. Yang, Z. Sheng, J. W. Wang, D. X. Dai, and S. L. He, "Compact 2×2 tapered multimode interference couplers based on SU-8 polymer rectangular waveguides," *Applied Physics Letters*, 2008, 93(20): 203304-1–203304-3.

[26] L. Jin, J. W. Wang, X. Fu, B. Yang, Y. C. Shi, and D. X. Dai, "High-Q microring resonators with 2 × 2 angled multimode interference couplers," *IEEE Photonics Technology Letter*, 2013, 25(6): 612–614.

[27] N. Xie, T. Hashimoto, and K. Utaka, "Design and performance of low-power, high-speed, polarization-independent and wideband polymer buried-channel waveguide thermo-optic switches," *Journal of Lightwave Technology*, 2014, 32(17): 3067–3072.

[28] J. L. Dong, K. S. Chiang, and W. Jin, "Compact three-dimensional polymer waveguide mode multiplexer," *Journal of Lightwave Technology*, 2015, 33(22): 4580–4588.

[29] H. B. Zhang, J. Y. Wang, L. K. Li, Y. Song, M. S. Zhao, and X. G. Jian, "A study on liquid hybrid material for waveguides-synthesis and property of PSQ-Ls for waveguides," *Journal of Macromolecular Science Part A*, 2008, 45(3): 232–237.

[30] X. Y. Han, L. H. Wang, Y. Wang, P. Zou, Y. Y. Gu, J. Teng, *et al*., "UV-soft imprinted tunable polymer waveguide ring resonator for microwave photonic filtering," *Journal of Lightwave Technology*, 2014, 32(20): 3924–3932.

[31] L. B. Soldano and E. C. M. Pennings, "Optical multi-mode interference devices based on self-imaging: principles and applications," *Journal of Lightwave Technology*, 1995, 13(4): 615–627.

[32] J. Wang, M. H. Qi, Y. Xuan, H. Y. Huang, Y. Li, M. Li, *et al*., "Proposal for fabrication-tolerant SOI polarization splitter-rotator based on cascaded MMI couplers and an assisted bi-level taper," *Optics Express*, 2014, 22(23): 27869–27879.

[33] K. Debnath, R. Moore, A. Liles, and L. O'Faolain, "Toolkit for photonic integrated circuits based on inverted rib waveguides," *Journal of Lightwave Technology*, 2015, 33(19): 4145–4150.